DYNAMIC MODEL OF FULL-SCALE MR DAMPERS FOR CIVIL ENGINEERING APPLICATIONS

G. YANG[1], H.J. JUNG[2] and B.F. SPENCER, Jr.[3]

[1] Doctoral Candidate, Department of Civil Engineering and Geological Sciences, University of Notre Dame, Notre Dame, IN 46556, USA, gyang2@nd.edu

[2] Postdoctoral Researcher, Department of Civil Engineering and Geological Sciences, University of Notre Dame, Notre Dame, IN 46556, hjung@nd.edu

[3] Linbeck Professor of Engineering, Department of Civil Engineering and Geological Sciences, University of Notre Dame, Notre Dame, IN 46556, spencer@nd.edu

ABSTRACT: Magnetorheological (MR) dampers are one of the most promising new devices for structural vibration reduction. Because of their mechanical simplicity, high dynamic range, low power requirements, large force capacity, and robustness, these devices have been shown to mesh well with application demands and constraints to offer an attractive means of protecting civil infrastructure systems against severe earthquake and wind loading. Quasi-static models of MR dampers have been investigated by several researchers. Although useful for design of the damper, quasi-static models are not sufficient to describe the MR damper behavior under dynamic loading. This paper presents a new dynamic model of the overall MR damper system which is comprised of two parts: (i) a dynamic model of the power supply, and (ii) a dynamic model of the MR damper. Because previous studies have demonstrated that a current driven power supply can dramatically reduce the MR damper response time, this study employs a current driver to power the MR damper. The operating principles of the current driver, and an appropriate dynamic model are provided. Subsequently, MR damper response analysis is performed, and a mechanical model using the Bouc-Wen model is proposed to predict the MR damper behavior under dynamic loading. This model accommodates MR fluid inertial and shear thinning effects. Experimental verification has shown that the proposed dynamic model of the MR damper system predicts the experimental results very well.

Key Words: MR fluids, MR dampers, Smart damping devices, Smart materials, Hysteresis model, Parameter estimation, System identification, Rheological technology

INTRODUCTION

Magnetorheological fluids (or simply “MR” fluids) belong to the class of controllable fluids. The essential characteristic of MR fluids is their ability to reversibly change from free-flowing, linear viscous liquids to semi-solids having a controllable yield strength in milliseconds when exposed to a magnetic field. This feature provides simple, quiet, rapid-response interfaces between electronic controls and mechanical systems. MR fluid dampers are new semi-active devices that utilize MR fluids to provide controllable damping forces. These devices overcome many of the expenses and technical difficulties associated with semi-active devices previously considered. Recent studies have shown that the semi-active dampers can achieve the majority of the performance of fully active systems, thus allowing for the possibility of effective response reduction during both moderate and strong seismic activity (Dyke et al.

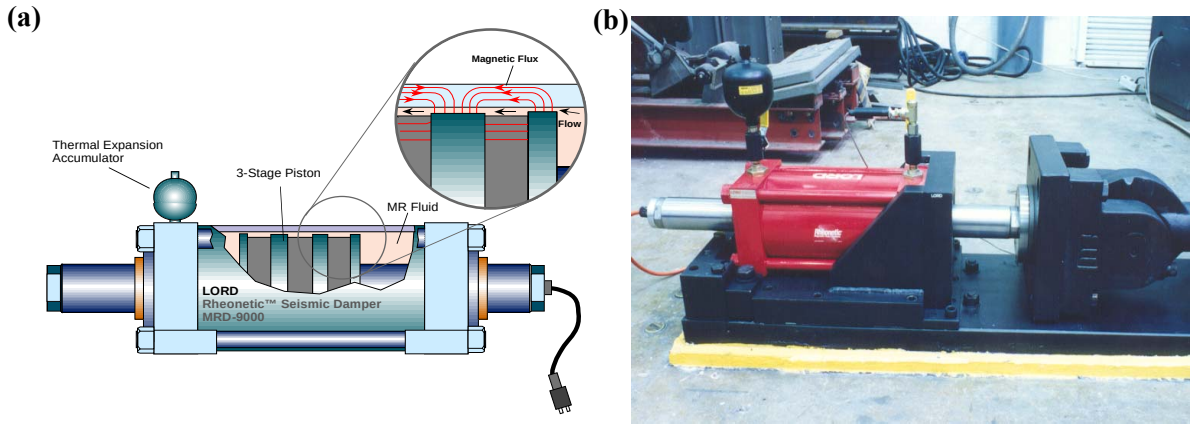

Fig. 1 (a) Schematic of the full-scale 20-ton MR fluid damper; (b) experimental setup.

1996; Jansen & Dyke 2000; Johnson et al. 2001; Spencer et al. 2000). For these reasons, significant efforts have been devoted to the development and implementation of MR devices.

To prove the scalability of MR fluid technology to devices of appropriate size for civil engineering applications, a full-scale 20-ton MR fluid damper has been designed and built (Spencer et al. 1998). Fig. 1a shows the schematic of the MR damper tested in this paper. The damper uses a particularly simple geometry in which the outer cylindrical housing is part of the magnetic circuit. The effective fluid orifice is the entire annular space between the piston outside diameter and the inside of the damper cylinder housing. The damper has an inside diameter of 20.3 cm and a stroke of ± 8 cm. The electromagnetic coils are wound in three sections on the piston, resulting in four effective valve regions as the fluid flows past the piston. The coils contain a total of about 1.5 km of wire. When wired in series, the total coil has an inductance $L_0 = 6.6$ H and a resistance $R_0 = 21.9\ \Omega$. The completed damper is approximately 1 m long and with a mass of 250 kg. The damper contains approximately 5 litres of MR fluid. The amount of fluid energized by the magnetic field at any given instant is approximately 90 cm^3. Fig. 1b shows the experimental setup at the University of Notre Dame for the full-scale 20-ton MR fluid damper. The damper was attached to a 7.5 cm thick plate that was grouted to a 2 m thick strong floor. The damper is driven by a 560 kN actuator configured with a 57 lpm servo-valve with a bandwidth of 30 Hz. The actuator is controlled by a Schenck-Pegasus 5910 servo-hydraulic controller in displacement feedback mode.

Quasi-static models of MR dampers have been developed by researchers (Gavin et al. 1996a; Kamath et al. 1996; Makris et al. 1996; Spencer et al. 1998; Wereley & Pang 1998; Yang et al. 2001). Although those models are useful for MR damper design, they are not sufficient to describe the MR damper nonlinear behavior under dynamic loading, especially the nonlinear force-velocity behavior. This paper presents a new dynamic model of the overall MR damper system which is comprised of two parts: (i) a dynamic model of the power supply, and (ii) a dynamic model of the MR damper. Because previous studies have demonstrated that a current driven power supply can dramatically reduce the MR damper response time, this study employs a current driver to power the MR damper. The operating principles of the current driver, and an appropriate dynamic model are provided. Subsequently, MR damper response analysis is performed, and a mechanical model using the Bouc-Wen model is proposed to predict the MR damper behavior under dynamic loading. This model accommodates MR fluid inertial and shear thinning effects. Experimental verification has shown that the proposed dynamic model of the MR damper system predicts the experimental results very well.

DYNAMIC MODEL OF CURRENT DRIVERS

The MR damper electromagnetic circuit (or damper coil) can be modeled using an electrical network in which a resistor and inductor are connected in series, as shown in Fig. 2 (Yang et al. 2001). The equation governing the current $i(t)$ in the coil is given by

$$L\frac{d}{dt}i(t) + R_L i(t) = V(t) = V_H\frac{T_{on}}{T} \tag{1}$$

where L and R_L = coil inductance and resistance, respectively; V_H = bus voltage; T_{on}/T = duty cycle; and $V = V_H(T_{on}/T)$ = equivalent output voltage of the PWM amplifier. Assuming a constant duty cycle T_{on}/T, the solution of Eq. (1) is

$$i(t) = \frac{V_H}{R_L}\frac{T_{on}}{T}\left(1 - e^{-\frac{R_L}{L}t}\right) = I_s\left(1 - e^{-\frac{R_L}{L}t}\right) \tag{2}$$

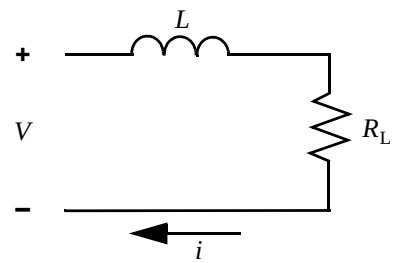

Fig. 2 Simple model of the electromagnet circuit.

Eq. (2) indicates that nearly $3L/R_L$ seconds are required for the current to reach 95% of the final value I_s, which is equal to $(V_H/R_L)(T_{on}/T)$. This exponential response is insufficient for many practical applications. Moreover, the fluctuation of power line voltage will affect the bus voltage V_H; this affects the steady state current I_s in the coils and thus the damper resisting force.

Several approaches can be considered to decrease the response time of the MR damper's magnetic circuit. One of them is to use a current driver instead of a voltage-driven power supply. The schematic of the current driver based on the PWM servo amplifier and its transfer function block diagram are given in Fig. 3. In order to obtain error-free control results, a PI controller is normally employed. Assuming that the duty cycle is proportional to the controller output u_c and that u_c is not saturated, Eq. (1) and the feedback loop

$$V(t) = \alpha V_H\left[K_i\int_0^t (v_0 - \beta i)dt + K_p(v_0 - \beta i)\right] \tag{3}$$

are combined to yield the governing equation for current driver as

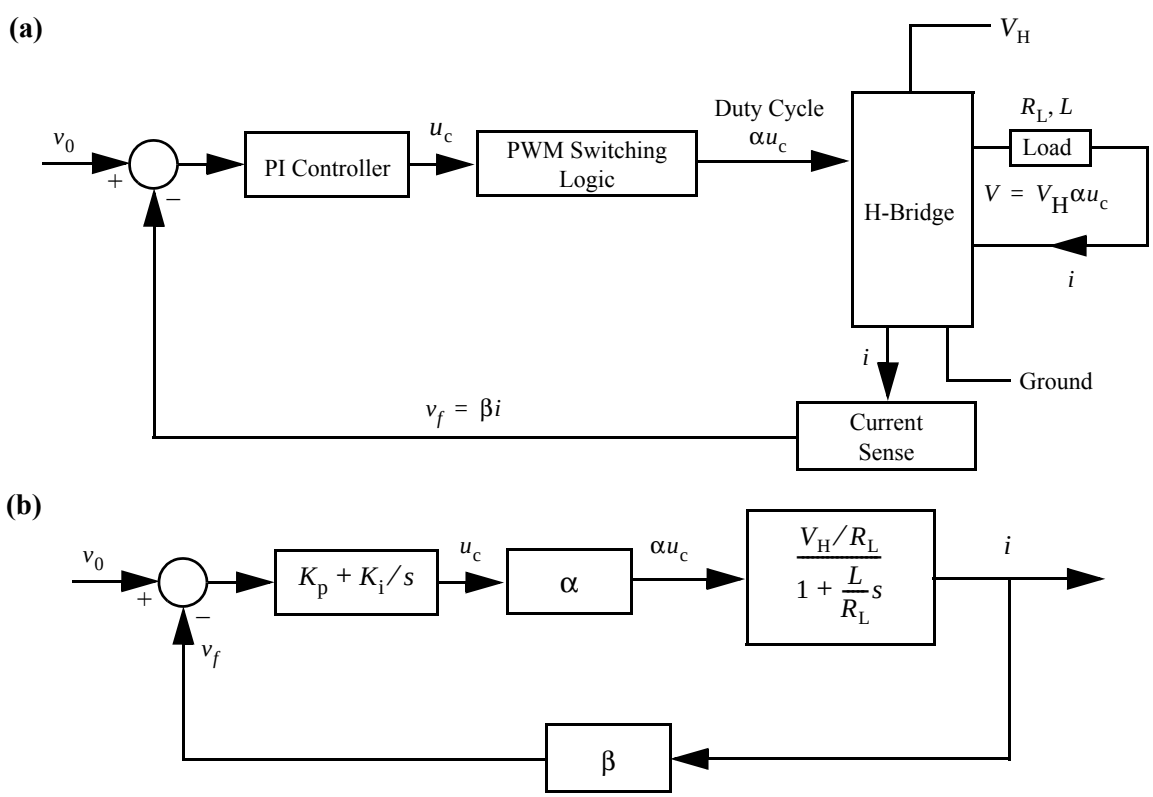

Fig. 3 (a) Schematic of the current driver based on the PWM servo amplifier; (b) transfer function block diagram of the current driver.

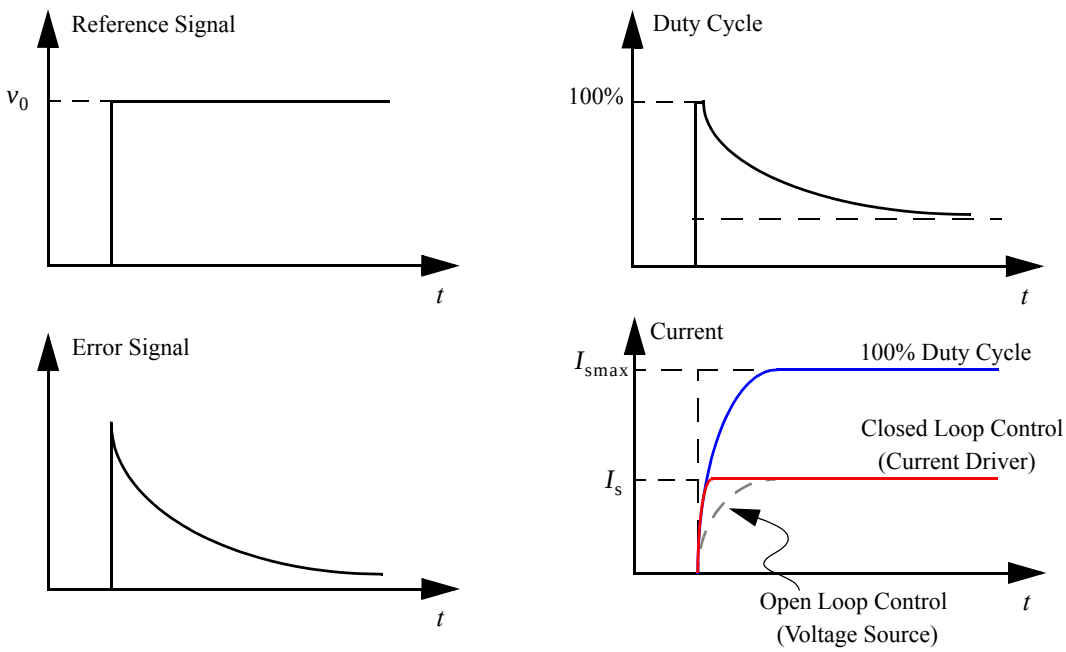

Fig. 4 Current driver response under a step reference signal.

$$\frac{L}{\beta\gamma}\frac{d^2 i}{dt^2} + \frac{(R_L + \beta\eta)}{\beta\gamma}\frac{di}{dt} + i = \frac{v_0}{\beta} + \frac{\eta}{\beta\gamma}\frac{dv_0}{dt} \tag{4}$$

where $\gamma = \alpha K_i V_H$; $\eta = \alpha K_p V_H$; v_0 = reference input signal; β = sensitivity of the current sensing; and K_p, K_i = controller proportional and integral gains. The steady state current is then given by

$$I_s = \frac{v_0}{\beta} \tag{5}$$

which depends only on the input reference signal v_0 and the sensitivity of the current sensing β. The load resistance R_L and the bus voltage V_H have no effect on the steady state current.

Fig. 4 shows a typical current driver response to a step reference signal. In order to achieve optimal performance, a relatively large proportional gain is used. Therefore, the controller output u_c is saturated at the beginning of the response, when the error signal is large. The power supply applies maximum voltage to facilitate the current increase, and the current is governed by Eq. (1). The current increase follows the same path as that of the 100% duty cycle. As the current increases, the error signal decreases. The controller output u_c is no longer saturated, and the current is governed by Eq. (4). The controller regulates the current to a steady state current of v_0/β. As compared with the exponential current response using a voltage source, the current driver can dramatically reduce the current response time which is readily seen in Fig. 4.

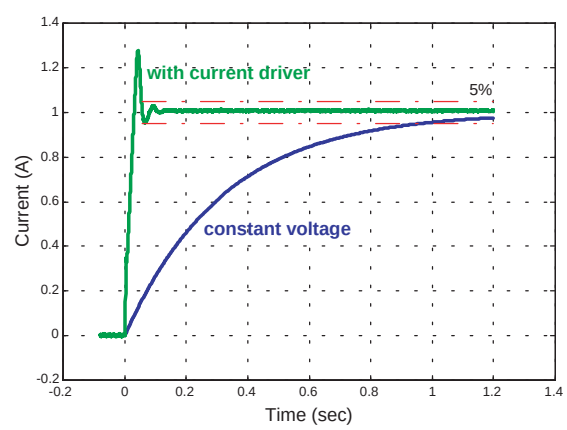

Fig. 5 Comparison between the coil current driven by constant voltage and current driver.

To experimentally verify the effectiveness of the current driver, currents in the 20-ton MR damper coil (connected in series) due to a step input command generated by both a constant voltage power supply and a current driver are compared. The experimental results are shown in Fig. 5 (Yang et al. 2000).

The constant voltage case corresponds to the scenario where a voltage-driven power supply is attached to the damper coils. The time constant L_0/R_0 for the coils of the 20-ton MR damper arranged in series is 0.3 sec. Therefore, as shown in Fig. 5, it takes about 1 sec for the current to achieve 95% of the final value, indicating that the damper has only a 1 Hz bandwidth. Alternatively, using a current driver, the 5% error range is achieved within 0.06 sec. The current driver includes a DC power supply (±120 V) and a PWM servo amplifier manufactured by Advanced Motion Controls operating under the current mode. Because the current driver clearly offers substantial reductions in the response time, the subsequent results reported in this paper will employ this current driver.

Based on Eq. (4), the dynamic model of the current driver used in the experiment is identified. The transfer function between the input reference signal v_0 and current i is given by

$$i(s) = \frac{1001.45s + 1016.1}{s^2 + 503.7s + 508.05} v_0(s) \tag{6}$$

A comparison between the measured and predicted current is provided in Fig. 6; close agreement is observed.

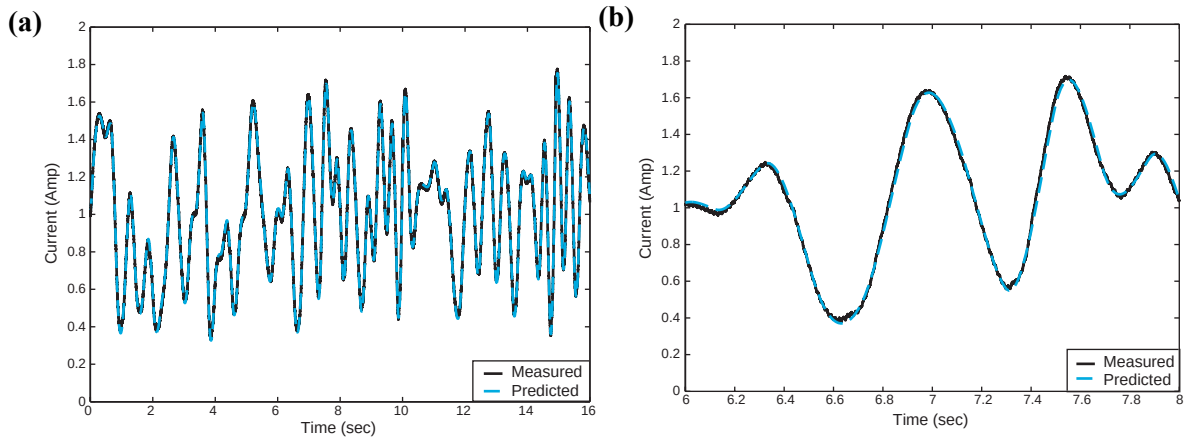

Fig. 6 (a) Comparison between the measured and predicted current; (b) detailed comparison in current fast-changing region.

DYNAMIC MODEL OF MR DAMPERS

MR damper response analysis

The response of the damper can basically be divided into three regions as shown in Fig. 7. At the beginning of region I, the velocity changes in sign from negative to positive, the velocity is quite small, and the MR fluid operates mainly in the pre-yield region, i.e., not flowing and having very small elastic deformation. Because the servo controller on the actuator driving the damper uses displacement feedback, and the displacement measurement at this stage is behind the command signal, the controller tends to command a large valve opening, subjecting the MR damper to a large force. Therefore, a substantial increase in acceleration is observed. After the MR fluid yields and the fluid begins to flow, the acceleration drops to its normal level, as shown at the end of region I. Because the inertial force is proportional to the acceleration, a force overshoot is observed, as shown in Fig. 7.

In region II, the acceleration decreases while still remaining positive; the velocity continues to increase. In general, the plastic-viscous force increases faster than the inertial force decreases. Therefore, a slight net force increase is observed.

In region III, both the velocity and acceleration decrease. Note that the damper velocity approaches zero at the end of this region, and the plastic viscous force drops more rapidly due to the fluid shear thinning effect. Therefore, a force roll-off is observed. Moreover, due to the inertial force, the damper resisting force in region III is smaller than in regions I and II. Therefore, there is a overshoot in the force, as shown in Fig. 8b.

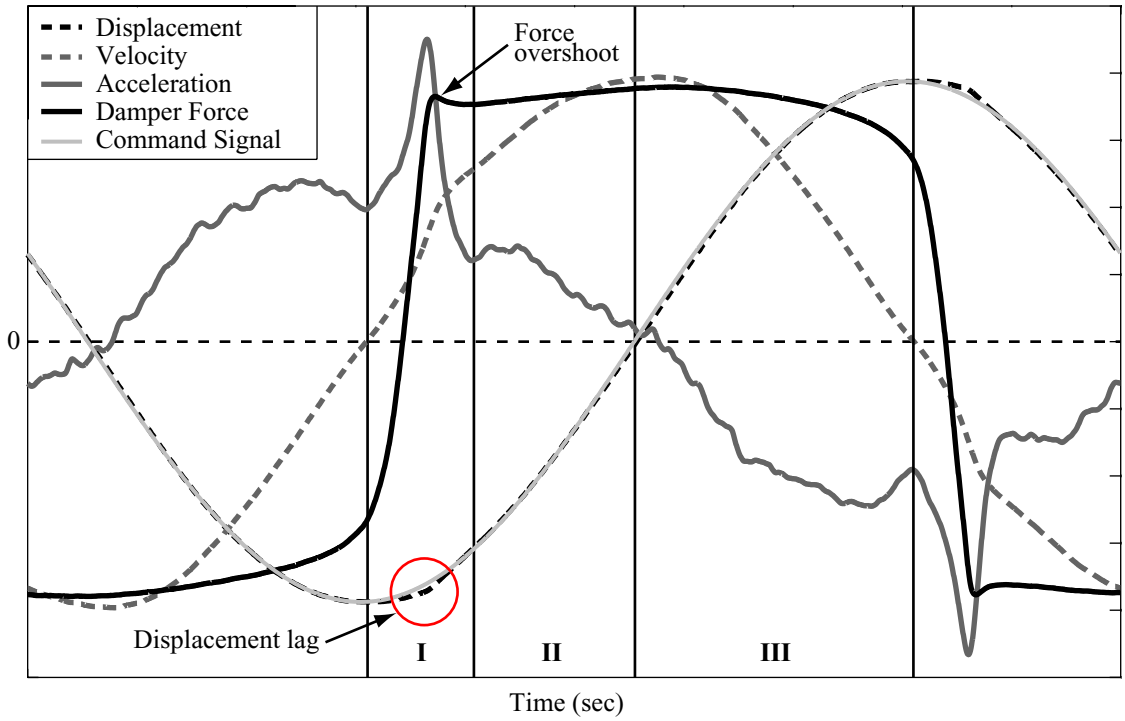

Fig. 7 MR damper response analysis.

Dynamic model of MR dampers

Quasi-static models for MR damper have been developed by researchers (Gavin et al. 1996a; Kamath et al. 1996; Makris et al. 1996; Spencer et al. 1998; Wereley & Pang 1998; Yang et al. 2001). Fig. 8 provides a comparison between the quasi-static model and experimental result when the MR damper is subjected to a 1 inch, 0.5 Hz sinusoidal displacement excitation at an input current of 2 A. It can be seen that quasi-static model can model the damper force-displacement behavior reasonably well; however, they are not sufficient to describe the nonlinear force-velocity behavior observed in the experimental data. A more accurate dynamic model of MR dampers is necessary for simulation of damper behavior and structural vibration control simulation with MR dampers.

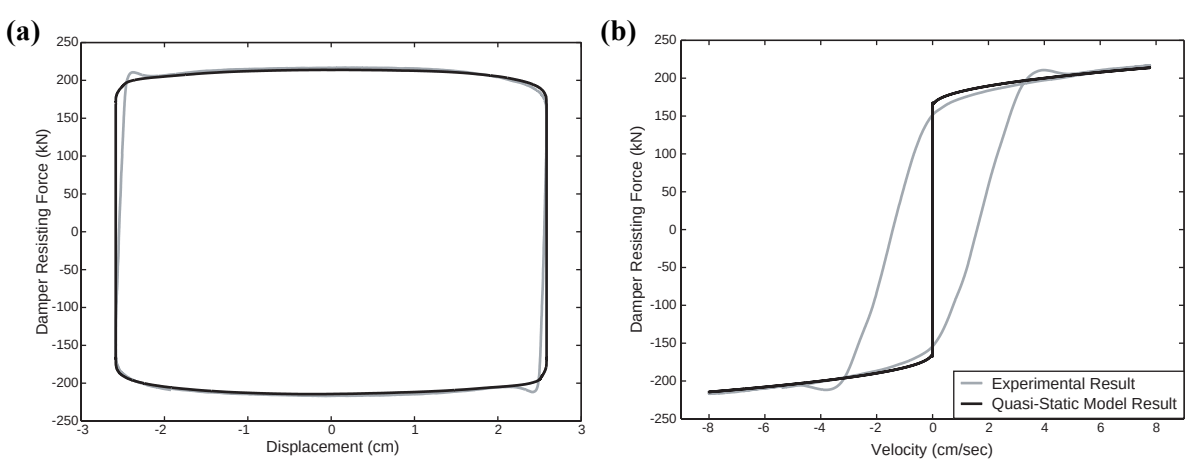

Fig. 8 Comparison between the quasi-static model and experimental results under an 1 inch, 0.5 Hz sinusoidal displacement excitation at an input current of 2 A, (a) force vs. displacement; (b) force vs. velocity.

Two types of dynamic models of controllable fluid damper have been investigated by researchers: non-parametric and parametric models. Ehrgott & Masri (1992) and Gavin et al. (1996b) presented a non-parametric approach employing orthogonal Chebychev polynomials to predict the damper resisting force using the damper displacement and velocity information. Chang & Roschke (1998) developed a neural network model to emulate the dynamic behavior of MR dampers. However, the non-parametric damper models are often quite complicated. Gamato & Filisko (1991) proposed a parametric viscoelastic-plastic model based on the Bingham model. Wereley et al. (1998) developed a nonlinear hysteretic biviscous model, which is an extension of the nonlinear biviscous model having an improved representation of the pre-yield hysteresis. Spencer et al. (1997) proposed a mechanical model based on the Bouc-Wen model. This model can well capture the force roll-off in the low velocity region due to bleed or blow-by of fluid between the piston and cylinder. Nevertheless, all parametric models mentioned above are not considered the fluid inertial effect and shear thinning effect especially in the low velocity region.

Based on the damper response analysis presented in the previous section, a mechanical model considering shear thinning and inertial effects is proposed which is shown in Fig. 9. The damper resisting force is given by

$$f = \alpha z + kx + c(\dot{x})\dot{x} + m\ddot{x} + f_0 \tag{7}$$

where the evolutionary variable z is governed by

$$\dot{z} = -\gamma|\dot{x}|z|z|^{n-1} - \beta\dot{x}|z|^n + A\dot{x} \tag{8}$$

In this model, the fluid inertial effect is represented by an equivalent mass m; the accumulator stiffness is represented by k; friction force due to the damper seals as well as measurement bias are represented by f_0; and the post-yield plastic damping coefficient is represented by $c(x)$. To describe the shear thinning effect on damper resisting force at low velocities as observed in the experimental data, $c(\dot{x})$ is defined as a mono-decreasing function with respect to the absolute velocity $|\dot{x}|$. In this paper, the post-yield damping coefficient is assumed to have a form of

$$c(\dot{x}) = a_1 e^{-(a_2|\dot{x}|)^p} \tag{9}$$

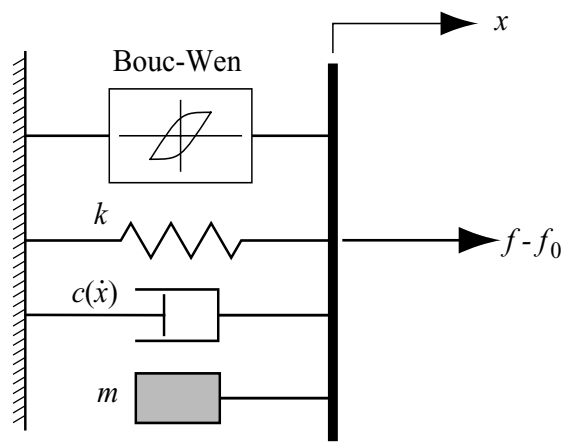

Fig. 9 Proposed mechanical model of MR dampers.

where a_1, a_2 and p are positive constants.

Besides the proposed mechanical model, two other types of dynamic models based on the Bouc-Wen model are also investigated. One is the simple Bouc-Wen model with mass element. Note that the damping coefficient is set to be a constant in this model. The other one is the mechanical model proposed by Spencer et al. (1997) with mass element. To assess their ability to predict the MR damper behavior, these three dynamic models are employed to fit to the damper response under a 1 inch, 0.5 Hz sinusoidal displacement excitation at an input current of 2A. The comparison between the predicted results and the experimental data is shown in Fig. 10. As can be seen, all models can describe the damper force-displacement behavior very well. However, the simple Bouc-Wen model fails to capture the force roll-off in the low velocity region. The mechanical model proposed by Spencer et al. (1997) utilizes two different damping coefficients to describe the force roll-off. One damping coefficient is used at large velocities, and the other is used at low velocities. As shown in the figure, this model has a slight, but not significant improvement over the simple Bouc-Wen model. The model proposed herein employs a variable mono-decreasing damping coefficient to describe the force roll-off due to the fluid shear thinning effect. It predicts the damper behavior very well in all regions, including the force roll-off at low velocities and two clockwise loops at velocity extremes. The parameters for the proposed mechanical model are chosen to be $\alpha = 927570$ N, $n = 2.7755$, $\gamma = 31778\ \mathrm{m}^{-1}$,

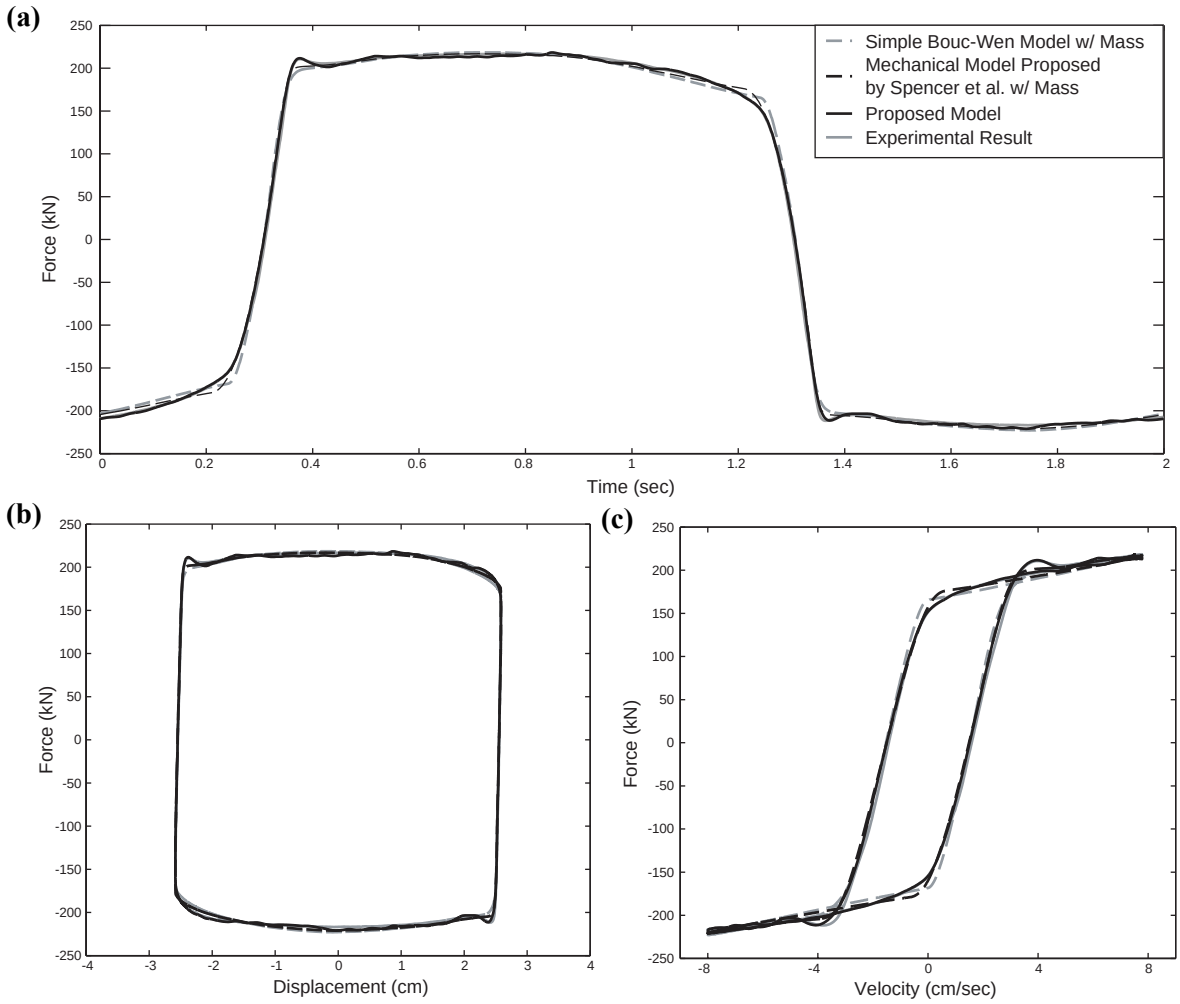

Fig. 10 Comparison between the predicted and experimentally-obtained responses with various dynamic models, (a) force vs. time; (b) force vs. displacement; (c) force vs. velocity.

$\beta = 21.637\ \mathrm{m}^{-1}$, $A = 217.27\ \mathrm{m}^{-1}$, $k = 486250\ \mathrm{N/m}$, $a_1 = 3308891\ \mathrm{N \cdot sec/m}$, $a_2 = 5.6809\ \mathrm{sec/m}$, $p = 0.5403$, $m = 59999\ \mathrm{kg}$, and $f_0 = -1377.32\ \mathrm{N}$.

In addition to the graphical evidence of the superiority of the proposed model, a quantitative study of the errors between each of the models and the experimental data is also explored. For each of the models considered herein, the error between the predicted force and the measured force has been calculated as a function of time, displacement and velocity over one complete cycle. The following expressions have been used to represent the errors (Spencer et al. 1997)

$$E_t = \frac{\varepsilon_t}{\sigma_f}, \qquad E_x = \frac{\varepsilon_x}{\sigma_f}, \qquad E_{\dot{x}} = \frac{\varepsilon_{\dot{x}}}{\sigma_f} \tag{10}$$

where

$$\varepsilon_t^2 = \frac{1}{T}\int_0^T (f_{\exp} - f_{\mathrm{pre}})^2 dt,\ \varepsilon_x^2 = \frac{1}{T}\int_0^T (f_{\exp} - f_{\mathrm{pre}})^2 \left|\frac{dx}{dt}\right| dt,\ \varepsilon_{\dot{x}}^2 = \frac{1}{T}\int_0^T (f_{\exp} - f_{\mathrm{pre}})^2 \left|\frac{d\dot{x}}{dt}\right| dt \tag{11}$$

$$\sigma_f^2 = \frac{1}{T}\int_0^T (f_{\exp} - \mu_F)^2 dt \tag{12}$$

The resulting error norms are given in Table 1. In all cases, the error norms calculated for the proposed mechanical model are smaller than those calculated for the other models considered, indicating that the proposed model is superior to the other models for the full-scale MR damper under investigation.

Generalization for fluctuating current

All of the data examined previously has been based on the response of the MR damper when the applied current, and hence the magnetic field, was held at a constant level. However, optimal performance of a control system using this device is expected to be achieved when the magnetic field is continuously varied based on the measured response of the system to which it is attached. To use the damper in this way, a model must be developed which is capable of predicting the behavior of the MR damper for a fluctuating current.

To determine a model which is valid under the fluctuating input current, the functional dependence of the parameters on the input current must be determined. Since the fluid yield stress is dependent on input current, α can then be assumed as a function of the input current i. Moreover, from the experiment results, a_1, a_2, m, n, and f_0 are also functions of the input current.

In order to obtain the relationship between the input current i and damper parameters α, a_1, a_2, n, m and f_0, the damper was driven by band-limited random displacement excitations with a cutoff frequency of 2 Hz at various constant current levels. A constrained nonlinear least-squares optimization scheme based on the trust-region and preconditioned conjugated gradients (PCG) methods is then used. The results are shown in Table 1. A linear piecewise interpolation approach is utilized to estimate these damper parameters for current levels which are not listed in the above table. The rest damper parameters which are not varied with input current are chosen to be $\gamma = 25179.04\ \mathrm{m}^{-1}$, $\beta = 27.1603\ \mathrm{m}^{-1}$, $A = 1377.9788\ \mathrm{m}^{-1}$, $k = 20.1595\ \mathrm{N/m}$, and $p = 0.2442$.

Table 1. Damper parameters at various current levels under random displacement excitation.

Current (A)	α (10^5 N)	a_1 ($\mathrm{N \cdot sec/m}$)	a_2 (sec/m)	m (kg)	n	f_0 (N)
0.0237	1.3612	4349000	862.03	3000	1.000	1465.82
0.2588	2.2245	24698000	3677.01	11000	2.0679	2708.36
0.5124	2.3270	28500000	3713.88	16000	3.5387	4533.98
0.7625	2.1633	32488000	3849.91	18000	5.2533	4433.08
1.0132	2.2347	24172000	2327.49	19500	5.6683	2594.41
1.5198	2.2200	38095000	4713.21	21000	6.7673	5804.24
2.0247	2.3002	35030000	4335.08	22000	6.7374	5126.79

Note that a first order filter needs to be used to accommodate the dynamics involved in the MR fluid reaching rheological equilibrium

$$H(s) = \frac{31.4}{s + 31.4} \tag{13}$$

Fig. 11 provides a comparison between the simulated force and the experimental data at a constant input current of 2 A. In this test, the damper is driven by a band-limited random displacement excitation with a cutoff frequency of 2 Hz. As seen here, the model accurately predicts the behavior of the damper. The error norms are determined to be $E_t = 0.09551$, $E_x = 0.00851$, and $E_{\dot{x}} = 0.02607$.

Furthermore, the predicted force is also compared with experimental data when the damper is subjected to a fluctuating current input. Similar to the previous test, a band-limited random displacement excitation is applied. The displacement excitation and input current is shown in Fig. 12. Again, excellent agreement is observed between the experimental and model responses. The error norms for this test are determined to be $E_t = 0.35517$, $E_x = 0.03257$, and $E_{\dot{x}} = 0.10118$.

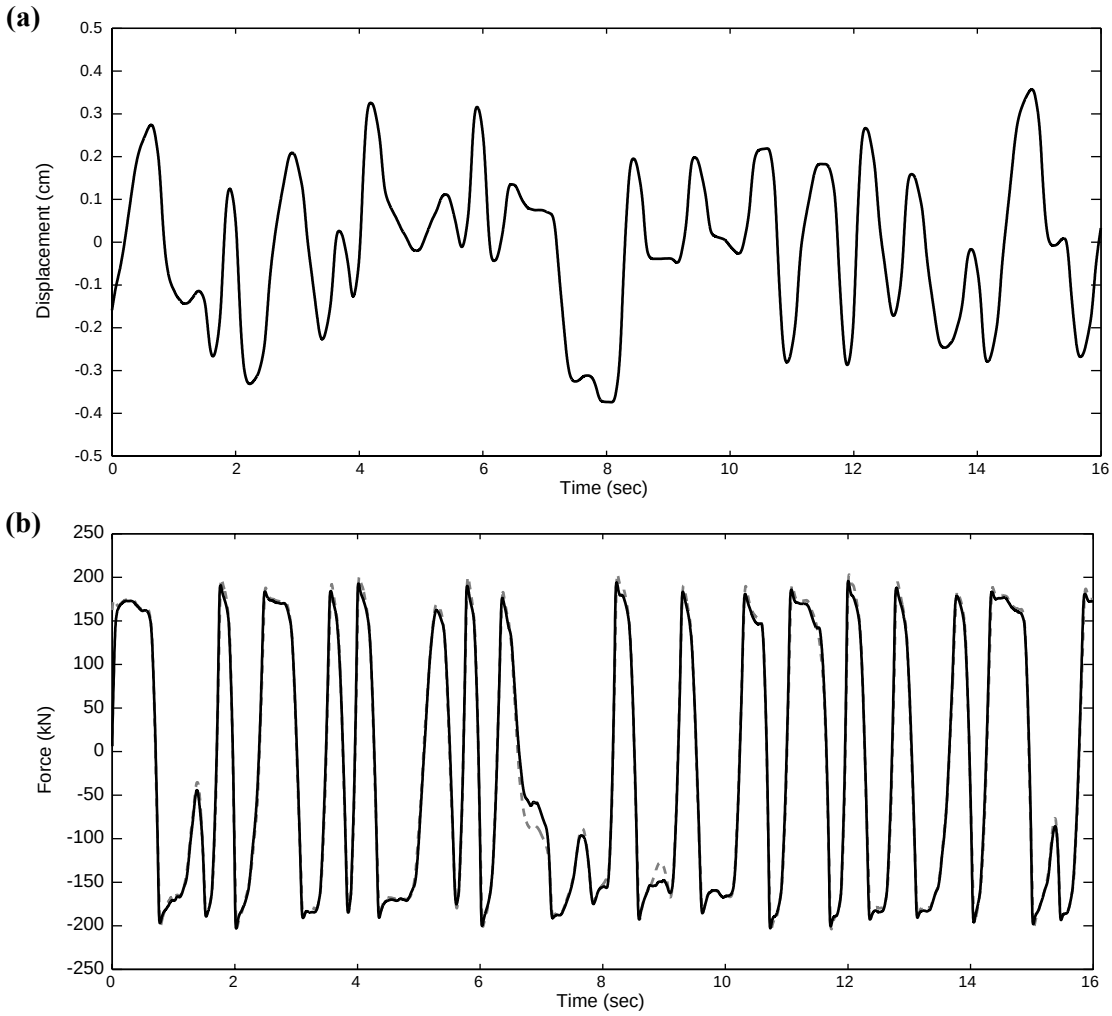

Fig. 11 Comparison between predicted and experimentally-obtain damper responses under random displacement excitation at constant input current of 2 A, (a) displacement vs. time; (b) force vs. time.

Fig. 13 illustrates the measured damper force upside using the force-feedback approach (Yang et al. 2001) and its comparison with predicted response. It can be seen that predicted result match very well with experimental data.

CONCLUSIONS

Magnetorheological (MR) fluid dampers provide a level of technology that has enabled effective semi-active control in a number of real world applications. A 20-ton MR damper capable of providing semi-active damping for full-scale structural applications has been designed and constructed.

A mechanical model based on the Bouc-Wen hysteresis model is proposed to describe the dynamic behavior of the MR damper. This model considers the fluid shear thinning and inertial effects which are observed in the experimental data. Moreover, experimental result also shows that current driver can dramatically reduce the MR damper response time. The operational principle of the current driver is also discussed and its dynamic model is given. This dynamic model is then combined with the mechanical model proposed for the MR damper to obtain the dynamic model of the overall MR damper system including the power supply. The predicted results are compared with experimentally-obtained data, and

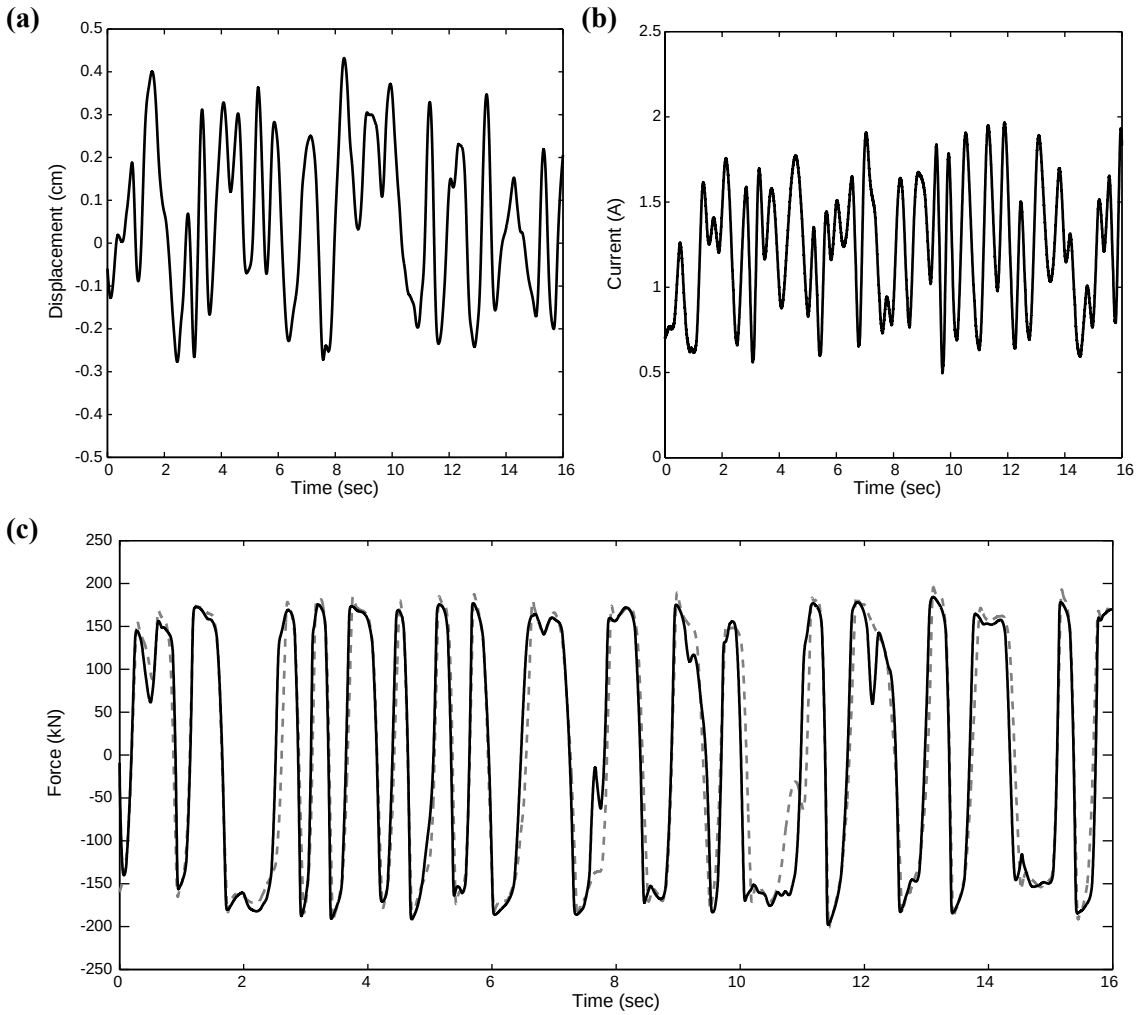

Fig. 12 Comparison between predicted and experimentally-obtained damper responses under random displacement excitation with random input current, (a) displacement vs. time; (b) current vs. time; (c) force vs. time.

excellent matches are observed. This model provides an excellent tool for analysis and synthesis of structures employing such large-scale controllable dampers.

ACKNOWLEDGEMENT

The authors gratefully acknowledge the support of this research by the National Science Foundation under grant CMS 99-00234 (Dr. S.C. Liu, Program Director) and Dr. J.D. Carlson at the LORD Corporation.

REFERENCES

Chang, C.C. & Roschke, P. (1998). Neural network modeling of a magnetorheological damper. *J. of Intelligent Material Systems and Structures,* 9:755–764.

Dyke, S.J., Spencer Jr., B.F., Sain, M.K. & Carlson, J.D. (1996). Modeling and control of magnetorheological dampers for seismic response reduction. *Smart Materials and Structures*, 5:565–575.

Ehrgott, R.C. & Masri, S.F. (1992). Modeling the oscillatory dynamic behavior of electrorheological materials in shear. *Smart Materials and Structures*, 1:275–285.

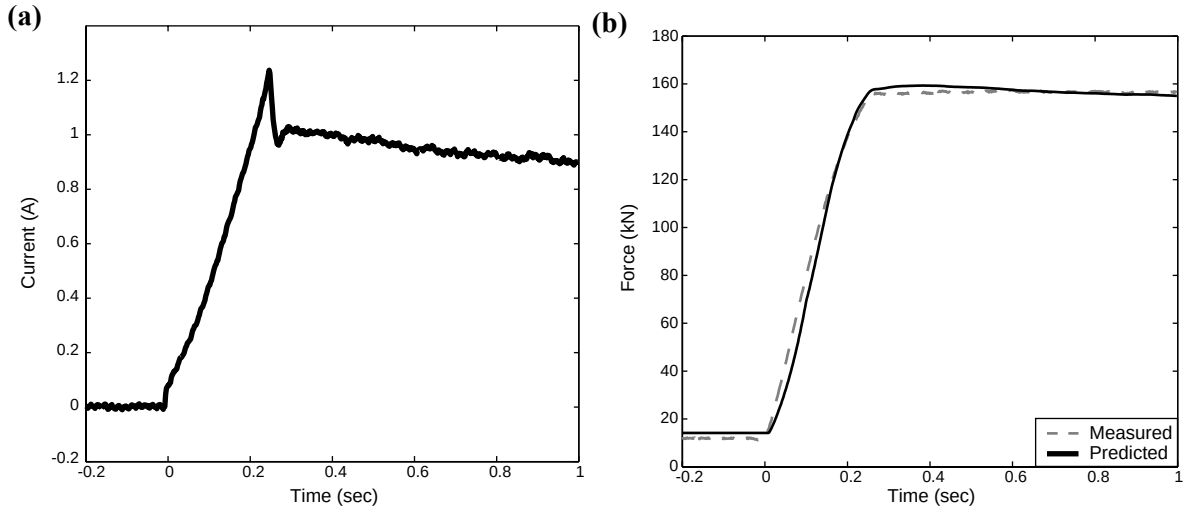

Fig. 13 Comparison between predicted and experimentally-obtained damper responses on force upside using force-feedback control (Yang et al. 2001), (a) current vs. time; (b) force vs. time.

Gamota, D.R. & Filisko, F.E. (1991). Dynamic mechanical studies of electrorheological materials: moderate frequencies. *J. of Rheology*, 35:399–425.

Gavin, H.P., Hanson, R.D. & Filisko, F.E. (1996a). Electrorheological dampers, part 1: analysis and design. *J. of Applied Mechanics*, ASME 63(9):669–675.

Gavin, H.P., Hanson, R.D. & Filisko, F.E. (1996b). Electrorheological dampers, part 2: testing and modeling. *J. of Applied Mechanics*, ASME 63(9):676–682.

Jansen, L.M. & Dyke, S.J. 2000. Semiactive control strategies for MR dampers: comparative study. *J. of Engineering Mechanics*, ASCE 126(8):795–803.

Johnson, E.A., Baker, G.A., Spencer Jr., B.F. & Fujino, Y. (2001). Semiactive Damping of Stay Cables. *J. of Engineering Mechanics*, ASCE, accepted.

Kamath, G.M., Hurt, M.K. & Wereley, N.M. (1996). Analysis and testing of Bingham plastic behavior in semi-active electrorheological fluid dampers. *Smart Materials and Structures*, 5:576–590.

Makris, N., Burton, S.A., Hill, D. & Jordan, M. (1996). Analysis and design of ER damper for seismic protection of structures. *J. of Engineering Mechanics*, ASCE 122(10):1003–1011.

Spencer Jr., B.F., Dyke, S.J., Sain, M.K. & Carlson. J.D. (1997). Phenomenological model of a magnetorheological damper. *J. of Engineering Mechanics*, ASCE 123(3):230–238.

Spencer Jr., B.F., Yang, G., Carlson, J.D. & Sain, M.K. (1998). "Smart" dampers for seismic protection of structures: a full-scale study. *Proceedings of 2nd World Conference on Structural Control*, Kyoto, Japan. pp. 417–426.

Spencer Jr., B.F., Johnson, E.A. & Ramallo, J.C. (2000). "Smart" isolation for seismic control. *JSME International Journal*, JSME 43(3):704–711.

Stanway, R., Sproston, J.L. & Stevens, N.G. (1987). None-linear modelling of an electro-rheological vibration damper. *J. of Electrostatics* 20:167–184.

Wereley, N.M. & Pang, L. (1998). Nondimensional analysis of semi-active electrorheological and magnetorheological dampers using approximate parallel plate models. *Smart Materials and Structures*, 7:732–743.

Wereley, N.M., Pang, L. & Kamath, G.M. (1998). Idealized hysteresis modeling of electrorheological and magnetorheological dampers. *J. of Intelligent Material, Systems and Structures*, 9(8):642–649.

Yang, G., Ramallo, J.C., Spencer Jr., B.F., Carlson, J.D. & Sain, M.K. (2000). Large-scale MR fluid dampers: dynamic performance considerations. *Proceedings of International Conference on Advances in Structure Dynamics*, Hong Kong, China. pp. 341–348.

Yang, G., Spencer Jr., B.F., Carlson, J.D. & Sain, M.K. (2001). Large-scale MR fluid dampers: modeling, and dynamic performance considerations. *Engineering Structures*, submitted.